Antiestrogen Binding Site and Estrogen Receptor Mediate Uptake and Distribution of 4-Hydroxytamoxifen-Targeted Doxorubicin−Formaldehyde Conjugate in Breast Cancer Cells

Patrick J. Burke,† Brian T. Kalet, and Tad H. Koch*

Department of Chemistry and Biochemistry, University of Colorado, Boulder, Colorado 80309

Received June 24, 2004

The anthracycline antitumor drug, doxorubicin (DOX), has long been used as a broad spectrum chemotherapeutic. The literature now documents the role of formaldehyde in the cytotoxic mechanism, and anthracycline−formaldehyde conjugates possess substantially enhanced activity in vitro and in vivo. We have recently reported the design, synthesis, and preliminary evaluation of a doxorubicin−formaldehyde conjugate targeted, via 4-hydroxytamoxifen, to the estrogen receptor (ER) and antiestrogen binding site (AEBS), which are commonly present in breast cancer cells. The lead targeted doxorubicin−formaldehyde conjugate, called DOX-TEG-TAM, was found to possess superior cell growth inhibition characteristics relative to clinical doxorubicin and an untargeted control conjugate, especially in ER-negative, multidrug resistant MCF-7/Adr cells. The enhanced activity in the absence of estrogen receptor raised the possibility that targeting was also mediated via AEBS. Fluorescence microscopy of an ER-negative, AEBS-positive cell line as a function of time showed initial DOX-TEG-TAM localization in cytosol, in contrast to initial DOX and untargeted doxorubicin−formaldehyde conjugate localization in the nucleus. DOX-TEG-TAM was taken up by four AEBS-positive cell lines to a greater extent than doxorubicin and an untargeted doxorubicin−formaldehyde conjugate. Of the four cell lines, three were ER negative. DOX-TEG-TAM uptake was inhibited in a dose-dependent manner by the presence of a competing AEBS ligand. DOX-TEG-TAM retains 60% of the affinity of 4-hydroxytamoxifen for AEBS. DOX-TEG-TAM was also taken up by the AEBS-negative, ER-positive cancer cell line Rtx-6; with these cells uptake was inhibited in a dose-dependent manner by the ER ligand, estradiol. The data support the hypothesis that uptake of 4-hydroxytamoxifen targeted doxorubicin−formaldehyde conjugate is mediated by both the antiestrogen binding site and estrogen receptor.

Introduction

For several decades the anthracycline antitumor drug, doxorubicin, has been employed in the treatment of breast cancer, the second leading cause of cancer-related death among women behind only lung cancer.[1] Doxorubicin exhibits a broad range of antineoplastic activity that has stimulated an immense research effort toward the elucidation of the cytotoxic mechanism and the development of superior doxorubicin derivatives.

While the anthracycline cytotoxic mechanism remains a matter of debate, DNA has clearly emerged as a target.[2,3] Anthracycline−DNA adducts have been correlated with cancer cell death,[4] and substantial evidence indicates that the drug−DNA lesion is mediated by a formaldehyde linkage.[5−10] Additionally, formaldehyde-releasing prodrugs have been shown to enhance the activity of doxorubicin.[11,12] Finally, anthracycline−formaldehyde conjugates have been shown to possess intriguing in vitro[13−15] and in vivo[16] activity.

We recently reported the design, synthesis, and preliminary evaluation of a class of doxorubicin−formaldehyde conjugates[17] targeted to the estrogen receptor (ER) and antiestrogen binding site (AEBS), proteins commonly present in large quantities in breast cancer cells. The targeting group was 4-hydroxytamoxifen (4-OHT), the active metabolite of the antiestrogen tamoxifen. At least two isoforms of the estrogen receptor have been identified, designated α and β. They are both expressed in MCF-7 breast cancer cells,[18] bind estradiol equally, and bind 4-OHT with comparable affinity.[19] Photoaffinity labeling experiments indicate that AEBS in liver microsomes consists of at least four proteins, three of which have been identified as microsomal epoxide hydrolase, carboxyesterase (ES10) and liver fatty acid binding protein (L-FABP), and all are involved in lipid metabolism.[20] Recent experiments indicate that two of the proteins of AEBS in MCF-7 cells are 3β-hydroxysterol-Δ^8-Δ^7-isomerase and 3β-hydroxysterol-Δ^7-reductase and that both are involved in cholesterol biosynthesis.[21]

The design of the targeted conjugates is shown in Figure 1. The formaldehyde function was incorporated in the form of an N-Mannich base joining the amide of a salicylamide moiety to the amine of doxorubicin.[22] The salicylamide moiety was used as a time-based chemical trigger to release the doxorubicin−formaldehyde conjugate, the presumed doxorubicin active metabolite, with a half-life for hydrolysis of about 60 min under physiological conditions.[15,22] The salicylamide trigger was tethered via ethylene glycol units to 4-hydroxyta-

* Author to whom correspondence should be addressed. Tel: 303-492-6193. Fax: 303-492-5894. E-mail: tad.koch@colorado.edu.
† Current address: Wayne State University, Department of Chemistry, Detroit, MI 48201.

10.1021/jm049496b CCC: $27.50
Published on Web 11/18/2004

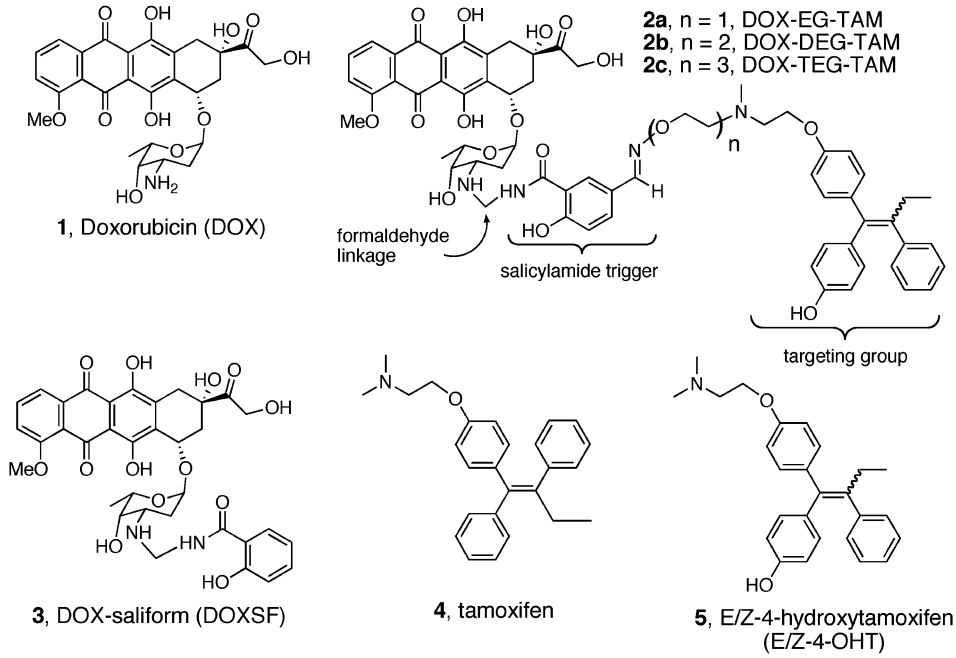

Figure 1. Structures of clinical DOX (**1**), targeted doxorubicin−formaldehyde conjugates (**2a**−**c**), untargeted DOX−saliform (**3**), clinical tamoxifen (**4**), and *E*/*Z*-4-hydroxytamoxifen targeting group (**5**).

Scheme 1. Synthesis of Hydroxytamoxifen-Targeted Doxorubicin−Formaldehyde Conjugates[a]

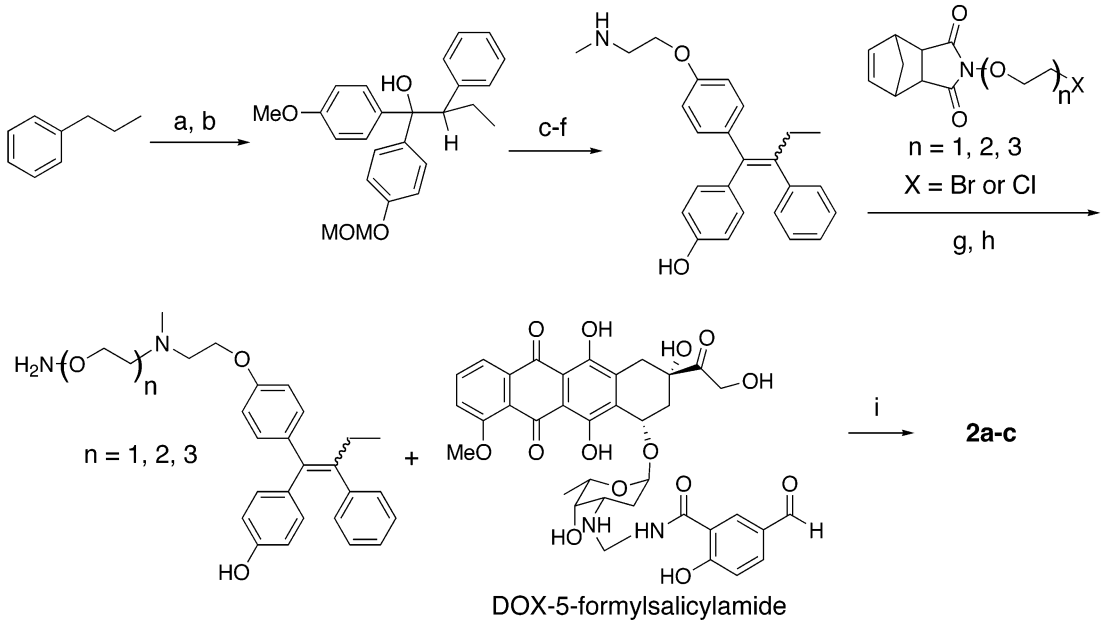

[a] Reagents and conditions: (a) n-BuLi, KOt-Bu, TMEDA; (b) 4-methoxy-4′-methoxymethylbenzophenone (97%); (c) 6 M HCl (93%); (d) $(n\text{-Bu})_4NHSO_4$, NaOH, 1,2-dibromoethane (90%), (e) BBr_3 (57%); (f) excess $MeNH_2$ (91%); (g) DIPEA (55−68%); (h) hydrazine (67−74%); (i) TFA, EtOH, water (∼50%).

moxifen, the active metabolite of tamoxifen. The targeting group was selected on the basis of its high binding affinity to ER and AEBS. An equimolar mixture of *E* and *Z* geometric isomers of 4-hydroxytamoxifen was utilized because previous work indicates that *p*-hydroxy-substituted triarylbutenes isomerize under cell culture conditions, compromising the interpretation of results with pure isomers.[23]

The synthesis of the targeted conjugates is shown in Scheme 1. Commercially available *n*-propylbenzene was metalated at the α position, and 4-methoxy-4′-methoxymethylbenzophenone was then added. The resulting carbinol was dehydrated and MOM-deprotected under acidic conditions. The free phenol was then bromoethylated via phase transfer conditions. Following removal of the methyl aryl ether with BBr_3, the primary bromide was aminated with excess methylamine, affording *E*/*Z*-desmethyl-4-hydroxytamoxifen. The resultant secondary amine was alkylated with norbornyl dicarboximide protected tethers. The norbornyl dicarboximide protecting group was then removed via hydrazinolysis to reveal the hydroxylamine ether functionality. Oximation with DOX-5-formylsalicylamide[17,22] proceeded under acidic conditions, providing **2a**−**c**. A detailed description of the synthesis has been reported.[17]

Table 1. Comparison of Growth Inhibition for Various Breast Cancer Cell Lines by Targeted and Untargeted Drugs as a Function of ER, MDR, and AEBS Expression[a]

cell line	ER/AEBS/MDR	DOX	DOXSF	DOX-TEG-TAM
MCF-7	+/+/−	200 ± 26	70 ± 5	30 ± 5
MCF-7/Adr	−/+/+	10000 ± 1300	2000 ± 320	60 ± 9
Rtx-6	+/−/−	200 ± 20	61 ± 8	67 ± 10
MDA-MB-231	−/+/−	300 ± 33	80 ± 9	30 ± 5
MDA-MB-435	−/+/−	150 ± 14	50 ± 9	40 ± 6

[a] IC_{50} values are reported in nM and represent the concentration of drug that inhibits 50% of the cell growth. IC_{50} values for MCF-7, MCF-7/Adr, MDA-MB-231, and MDA-MB-435 cells were reported earlier.[17] IC_{50} values for Rtx-6 cells were determined as described in the Experimental Section.

Preliminary biological evaluation identified DOX-TEG-TAM (**2c**), the conjugate containing the triethylene glycol derived tether, as the lead compound.[17] DOX-TEG-TAM was more cytotoxic than DOX (**1**) and untargeted control conjugate DOX−saliform (**3**, DOXSF) in all four breast cancer cell lines tested, regardless of ER and multidrug resistance (MDR) expression. Structures for all compounds are shown in Figure 1. The most dramatic enhancement in activity for DOX-TEG-TAM relative to DOX and DOXSF was observed in MCF-7/Adr cells, an ER-negative breast cancer cell line that expresses MDR.[24] DOX-TEG-TAM was 140-fold and 28-fold more cytotoxic to MCF-7/Adr cells than DOX and DOXSF, respectively, as summarized in Table 1. MCF-7/Adr cells are a doxorubicin (trade name Adriamycin) resistant variant of MCF-7 cells. In addition to growth inhibition assays, the targeted conjugates' ER binding affinity was investigated. DOX-TEG-TAM retained 2.5% of the ER binding affinity relative to targeting group alone.

The dramatic enhancement in growth inhibition of the targeted doxorubicin−formaldehyde conjugates in MCF-7/Adr cells relative to doxorubicin and untargeted DOX−saliform cannot be explained in terms of targeting the ER; MCF-7/Adr cells are ER negative.[25] These observations raise the possibility that targeting is occurring, at least in part, through binding interaction with AEBS. The AEBS targeting hypothesis is as follows: (1) the targeted conjugates (**2a**−**c**) passively diffuse across the cytoplasmic membrane, (2) the targeting group binds to cytosolic AEBS, (3) the AEBS serves to sequester the conjugate, preventing drug efflux by the p-glycoprotein drug efflux pump (expressed as part of the MDR phenotype in MCF-7/Adr cells), and (4) the trigger fires, releasing the doxorubicin active metabolite, which then intercalates and alkylates DNA, leading to cell death. On the other hand, in the case of doxorubicin and DOXSF, following diffusion across the cell membrane, the p-glycoprotein efflux pump would rapidly transport them out of the MCF-7/Adr cells.

As a means to address the validity of the hypothesis, we performed a series of experiments to measure the uptake and retention of the lead compound, DOX-TEG-TAM (**2c**), relative to doxorubicin and untargeted DOXSF. The cellular accumulation of drug was observed by tracking the presence of the anthraquinone fluorophore via flow cytometry. Enhanced accumulation of targeted conjugate relative to controls would suggest effective targeting. Furthermore, uptake of the targeted conjugate should be reduced in the presence of a competing ligand if targeting is mediated by an AEBS binding interaction.

The reliance on anthracycline fluorescence to quantify cell uptake is complicated by the effect of local environments on the anthracycline fluorophore. For example, drug fluorescence is enhanced in lipid membranes[26] and partially quenched by drug−DNA intercalation.[27,28] However, cellular doxorubicin fluorescence has been shown to increase in a time- and dose-dependent manner;[29] as well, cell growth inhibition is directly correlated with doxorubicin fluorescence.[30] Therefore, drug fluorescence provides a reliable indication of the relative degree of drug uptake and retention.

In addition to flow cytometry, fluorescence microscopy was utilized to assess the cellular distribution of doxorubicin fluorophore following treatment with targeted conjugate and untargeted controls. If the targeted conjugate experiences binding to extranuclear AEBS as part of the mechanism, the drug should appear cytosolic following short (5−60 min) treatment times, prior to trigger hydrolysis.

We now report that DOX-TEG-TAM is taken up and retained by AEBS-positive MCF-7, MCF-7/Adr, MDA-MB-231, and MDA-MB-435 cancer cell lines to a greater extent than clinical DOX and untargeted DOXSF. Furthermore, DOX-TEG-TAM uptake in MDA-MB-435 cells is reduced in the presence of tamoxifen, as a competing ligand, in a dose-dependent manner. DOX-TEG-TAM appears cytosolic by fluorescence microscopy after short treatment times (5−60 min) in contrast to DOX and DOXSF, which both appear nuclear. DOX-TEG-TAM retains 63% of the AEBS binding affinity relative to the targeting group alone. DOX-TEG-TAM is also taken up by AEBS-negative, ER-positive, Rtx-6 cells, but with these cells uptake is inhibited by the ER specific ligand estradiol. These data support a targeting mechanism mediated by AEBS as well as ER.

Results and Discussion

Uptake and Release of DOX-TEG-TAM. The uptake of 500 nM DOX, DOXSF, and DOX-TEG-TAM following treatment for various times up to 1 h was assessed by flow cytometry. Uptake beyond that treatment time was not explored since the half-life for hydrolysis of the formaldehyde conjugates is 1 h.[17] The release of drugs following a 500 nM treatment for 1 h was assessed at various times out to 6 h posttreatment. Resistant MCF-7/Adr cells were first assessed as they provide a means to evaluate the AEBS targeting hypothesis (above) to explain the dramatic improvement in tumor cell growth inhibition observed for DOX-TEG-TAM relative to DOXSF and clinical DOX. The uptake in MCF-7/Adr cells following treatment for 20, 40, and 60 min with 500 nM DOX, DOXSF, or DOX-TEG-TAM is shown in Figure 2, panel A. DOX and DOXSF were taken up by the cells to the extent of one relative fluorescent unit (RFU), while DOX-TEG-TAM was taken up almost twice as much. Drug release for all three compounds was observed at 0.5, 1, 3, and 6 h following a 1 h treatment with 500 nM of each cytotoxin. In all three cases the drug fluorescence decreased dramatically up to 1 h posttreatment, as free drug was transported from the cell. At 6 h posttreatment DOX-TEG-TAM maintained a higher level of drug retention

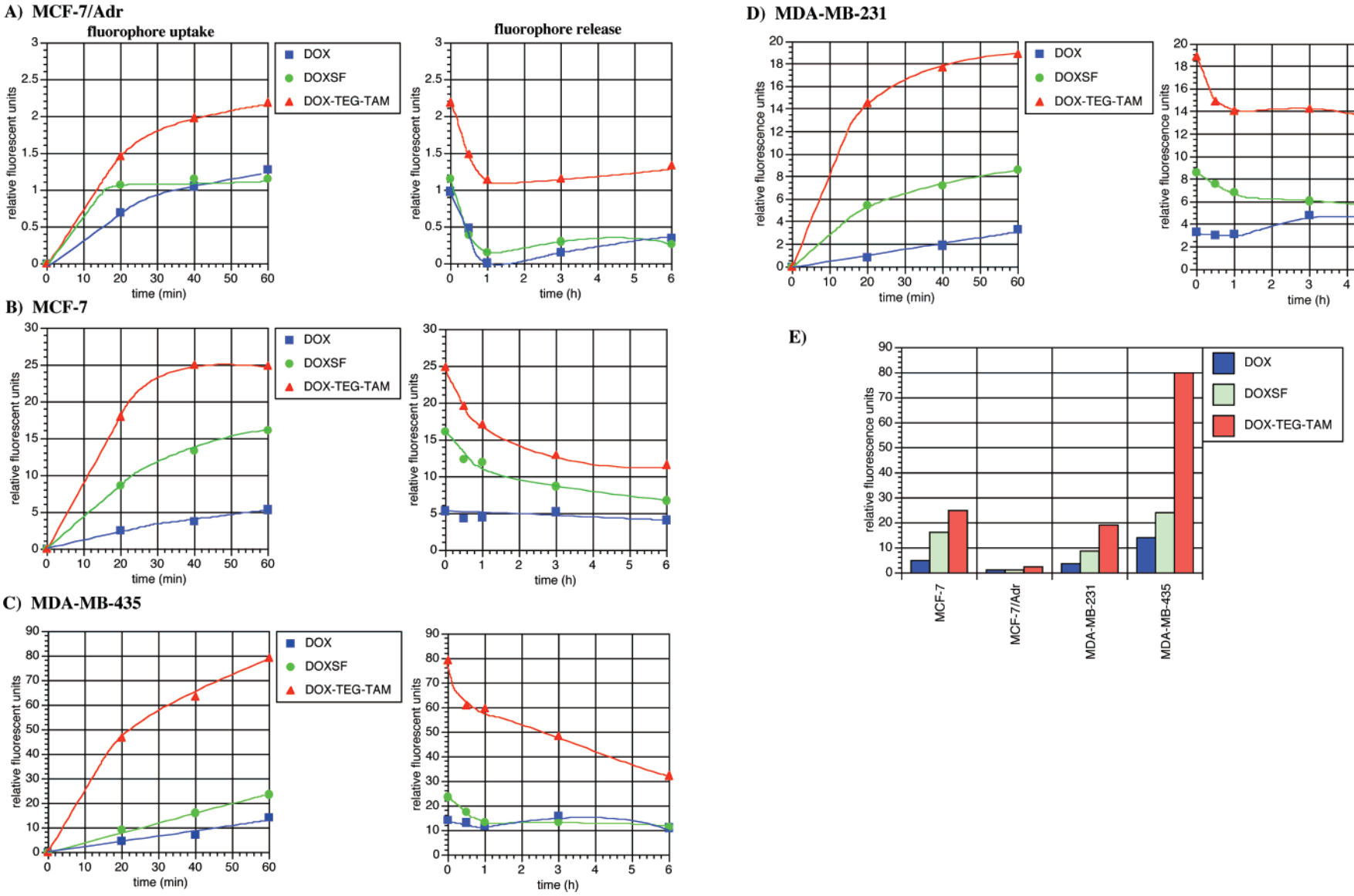

Figure 2. (A−D) Cellular uptake and release of drug following treatment with 500 nM DOX, DOXSF, or DOX-TEG-TAM as a function of time, measured by flow cytometric monitoring of fluorescence from the DOX fluorophore. (E) Relative uptake after 1 h of drug treatment.

relative to DOX and DOXSF. The enhanced uptake and retention of DOX-TEG-TAM relative to DOX and DOXSF parallels the growth inhibition data shown in Table 1[17] and provides evidence in favor of the targeting hypothesis involving interaction with AEBS.

The uptake and release of DOX, DOXSF, and DOX-TEG-TAM in ER-positive, drug sensitive MCF-7 cells is shown in Figure 2, panel B. DOX-TEG-TAM was taken up to a greater extent (25 RFU) than both DOXSF (16 RFU) and DOX (5 RFU). DOX-TEG-TAM showed the highest level of doxorubicin fluorophore retention following drug release after 6 h. Again, the uptake and retention parallel the growth inhibition data for DOX, DOXSF, and DOX-TEG-TAM (Table 1).[17]

Additionally, uptake and release data were obtained for DOX, DOXSF, and DOX-TEG-TAM in ER-negative MDA-MB-435 (Figure 2, panel C) and MDA-MB-231 cells (Figure 2, panel D). In both cell lines DOX-TEG-TAM was also taken up to a much greater extent than DOX and DOXSF. In MDA-MB-435 cells DOX-TEG-TAM was taken up 3-fold and 5-fold more than DOXSF and DOX, respectively. In MDA-MB-231 cells DOX-TEG-TAM was taken up 2-fold and 6-fold more than DOXSF and DOX, respectively. In both cell lines doxorubicin fluorophore, following 1 h treatment with 500 nM DOX-TEG-TAM, was retained to a greater extent than it was following treatment with 500 nM DOXSF or DOX.

The comparison of the extent of DOX-TEG-TAM uptake as a function of breast cancer cell type is shown graphically in Figure 2, panel E. The data illustrate that MDA-MB-435 cells take up substantially more drug following a 1 h treatment with 500 nM DOX-TEG-TAM. MCF-7 and MDA-MB-231 cells take up about 25% relative to MDA-MB-435 cells; while MCF-7/Adr cells, consistent with the overexpression of the p-glycoprotein drug efflux pump, take up a relatively small amount of drug. The enhanced uptake of DOX-TEG-TAM in MDA-MB-435 cells relative to MCF-7 and MDA-MB-231 cells was not anticipated based on growth inhibition data, as the IC_{50}s for all three cell lines following 4 h DOX-TEG-TAM treatment are quite similar (30−40 nM) (Table 1).[17]

Competitive Inhibition of Drug Uptake. If DOX-TEG-TAM targeting is AEBS mediated, the presence of a competitive ligand should inhibit uptake. MDA-MB-435 cells were utilized for competition experiments as they take up all three compounds to a greater extent than the other breast cancer cells evaluated (Figure 2, panel E). MDA-MB-435 cells were treated with 0.5 μM DOX-TEG-TAM, DOX, or DOXSF for 1 h in the presence of various concentrations of tamoxifen. In the presence of 10 μM tamoxifen competitor, the uptake of DOX and DOXSF relative to DOX-TEG-TAM decreased by only 8% and 6%, respectively, while in the case of cells treated with DOX-TEG-TAM, uptake of targeted drug decreased dramatically in a dose-dependent manner as shown in Figure 3. At 10 μM tamoxifen, the uptake was 47% of the uptake of DOX-TEG-TAM in the absence of competitor, supporting the hypothesis that DOX-TEG-TAM targeting is AEBS mediated.

Analysis of Drug Distribution by Fluorescence Microscopy. If drug targeting is mediated by extranuclear AEBS, the cellular distribution of doxorubicin

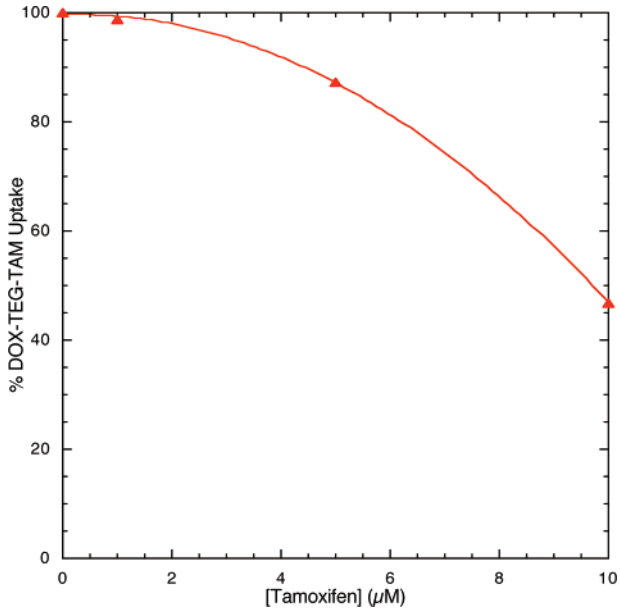

Figure 3. Drug uptake in MDA-MB-435 cells following 1 h treatment with 0.5 μM DOX-TEG-TAM in the presence of increasing concentration of tamoxifen as measured by fluorescence from the DOX fluorophore.

fluorophore following treatment with DOX-TEG-TAM should be predominantly cytosolic following short treatment times (treatment time less than the half-life for hydrolysis). Furthermore, once the trigger has fired, the DOX fluorophore should appear nuclear. DOX was used as a control since, with DOX treatment, drug fluorescence typically appears nuclear as the clinical drug accumulates in nuclear DNA.[29,31]

Fluorescence micrographs of MDA-MB-435 cells following treatment with 500 nM DOX or 500 nM DOX-TEG-TAM as a function of time are shown in Figure 4. Following treatment for 5 min, almost no fluorescence was observed for the DOX treated cells (column A, Figure 4) and very little was observed for DOX-TEG-TAM cells (column B, Figure 4). However, after 20 min, DOX fluorophore was observed in the nucleus of the cells following treatment with DOX, while cytosolic fluorescence was observed for DOX-TEG-TAM treated cells. Following 40 min of treatment, the DOX treated cells were observed to have accumulated more nuclear fluorophore. However, in the cells treated with DOX-TEG-TAM for 40 min the fluorescence still appeared extranuclear; however, the fluorophore appeared to have localized at a cytosolic site. The observed localization of DOX-TEG-TAM fluorophore appeared even more dramatic following treatment for 1 h. Following DOX treatment for 1 and 3 h, the fluorescence continued to appear exclusively nuclear. Following DOX-TEG-TAM treatment for 3 h, the fluorescence appeared predominantly nuclear. This is consistent with the observation that the half-life for hydrolysis of the trigger is about 60 min; after three half-lives the majority of the DOX-TEG-TAM should have hydrolyzed from the targeting group and the liberated doxorubicin active metabolite translocated to the nucleus, forming DNA *virtual cross-links*.[32] In an additional control experiment, untargeted DOXSF was found to mimic the localization pattern (exclusively nuclear) that was observed for DOX (data not shown).

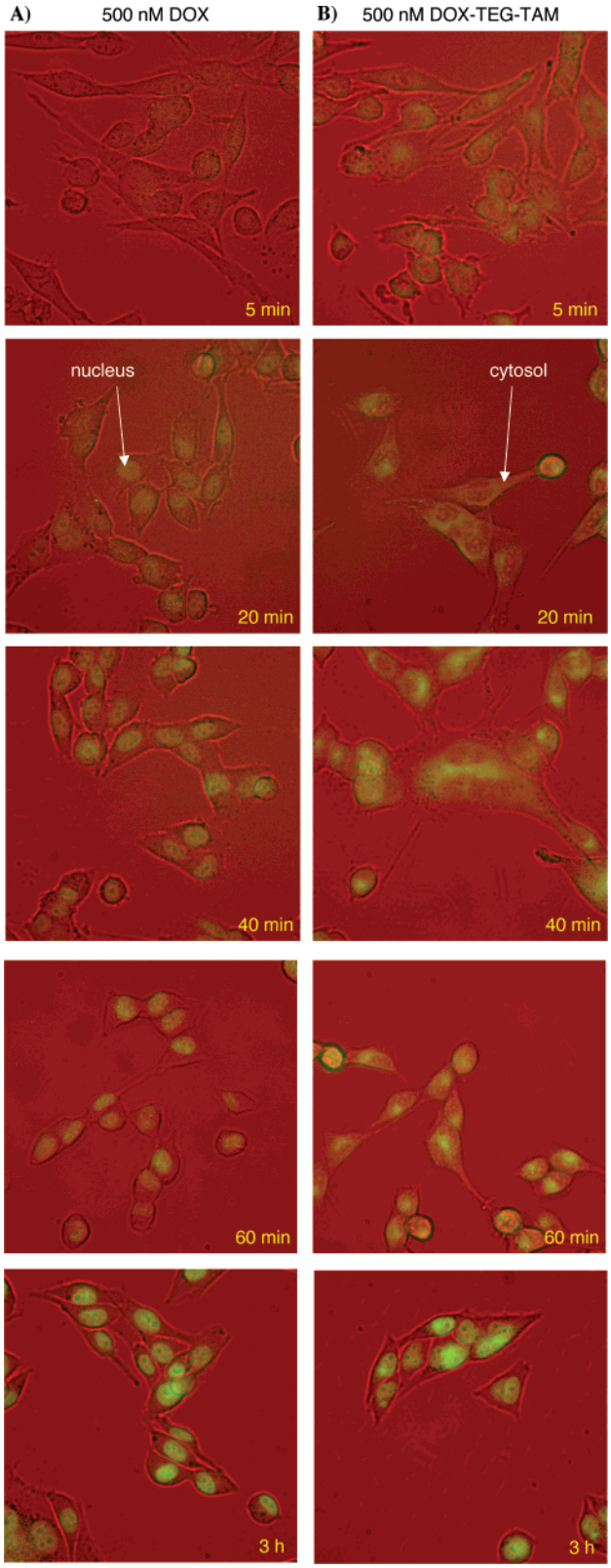

Figure 4. Fluorescence micrographs of MDA-MB-435 cells as a function of time following treatment with 500 nM DOX (A) and 500 nM DOX-TEG-TAM (B).

DOX-TEG-TAM Binding Affinity to AEBS. The binding affinity of DOX-TEG-TAM relative to *E*/*Z*-4-OHT was determined using MCF-7 cell lysate as an AEBS source. The lysate was incubated with ^{3}H-tamoxifen and cold competitors; 1000 nM estradiol was added to saturate ERs present in the cell lysate.

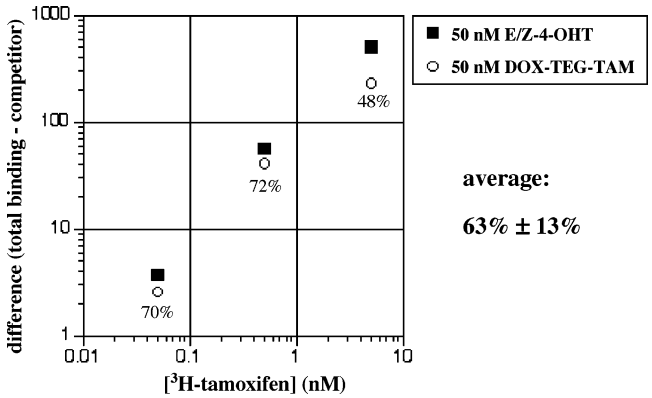

Figure 5. Binding affinity of DOX-TEG-TAM for AEBS relative to *E*/*Z*-hydroxytamoxifen.

Following incubation, free, unbound tamoxifen was stripped from solution with 2% dextran-coated charcoal (DCC) buffered suspension; bound ^{3}H-tamoxifen in solution was then quantified via scintillation counting. Representative results are shown in Figure 5. Three concentrations of ^{3}H-tamoxifen binding in the presence of 50 nM competitor were subtracted from total ^{3}H-tamoxifen binding (no competitor); the differences are plotted versus the concentration of ^{3}H-tamoxifen in Figure 5. Theoretically, a compound (competitor) with no AEBS affinity would result in no difference between total binding and competitor. At all three concentrations of ^{3}H-tamoxifen, DOX-TEG-TAM binding affinity was less than that of the targeting group alone. DOX-TEG-TAM binding affinity was 70%, 72%, and 48% relative to the targeting group (**5**) at 0.05 nM, 0.5 nM, and 5 nM ^{3}H-tamoxifen, respectively. Taken as an average, DOX-TEG-TAM (**2c**) retains 63% ± 13% of the total binding affinity of the targeting group, *E*/*Z*-4-OHT (**5**).

Effect of DOX-TEG-TAM on AEBS-Negative Rtx-6 Breast Cancer Cells. Rtx-6 cells, kindly provided by Dr. Marc Poirot (Toulouse, France), were evaluated as an AEBS-negative control cell line. Rtx-6 cells, a tamoxifen resistant breast cancer cell line, are a clonal variant of MCF-7 cells.[33−35] The Rtx-6 cells were utilized to determine the effect of the absence of AEBS on the cytotoxicity and uptake of DOX, DOXSF, and DOX-TEG-TAM.

Rtx-6 cells, in logarithmic growth, were treated with DOX, DOXSF, or DOX-TEG-TAM to establish the concentration that inhibited 50% of cell growth (IC_{50}) following a 4 h treatment. The IC_{50}s are compared in Table 1 with those previously determined for MCF-7, MCF-7/Adr, MDA-MB-231, and MDA-MB-435 cells. The concentrations inhibiting 50% of cell growth following 4 h treatment with DOX, DOXSF, and DOX-TEG-TAM were 200 nM, 61 nM, and 67 nM, respectively.

The uptake and release in Rtx-6 cells were also investigated. Rtx-6 cells were treated with DOX, DOXSF, or DOX-TEG-TAM as described above to determine both the uptake and the release of drug following a 1 h treatment. The results are shown in Figure 6. DOX-TEG-TAM was taken up to a greater extent than DOX (>3-fold) and DOXSF (>2-fold). The enhanced uptake relative to DOX and DOXSF could be attributed to the presence of ER and the lipophilicity of DOX-TEG-TAM. The uptake of DOX-TEG-TAM in Rtx-6 cells is perhaps best compared to the uptake in the parent MCF-7 cell

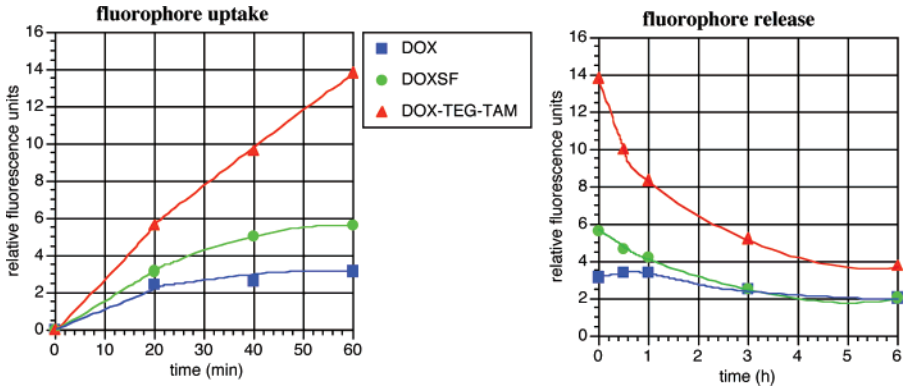

Figure 6. Flow cytometric measurement of cellular uptake and release in Rtx-6 cells following treatment with 500 nM DOX, DOXSF, and DOX-TEG-TAM as a function of time.

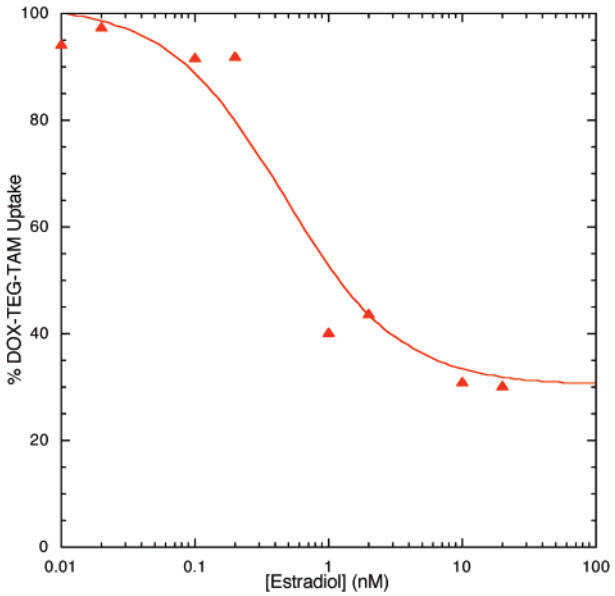

Figure 7. Drug uptake in Rtx-6 cells following 1 h treatment with 500 nM DOX-TEG-TAM in the presence of increasing concentration of estradiol, measured by flow cytometric monitoring of fluorescence from the DOX fluorophore.

line. DOX-TEG-TAM was taken up to a greater extent in MCF-7 cells (25 RFU) relative to Rtx-6 cells (14 RFU). One possible explanation for this difference is the presence of both AEBS and ER in MCF-7 cells versus only ER in Rtx-6 cells. Consistent with this explanation is the dose-dependent inhibition of uptake of DOX-TEG-TAM by the ER specific ligand, estradiol shown in Figure 7. Estradiol at 20 nM inhibited the uptake by 70%. No further inhibition occurs at higher concentrations, possibly because of nonspecific binding of DOX-TEG-TAM at hydrophobic sites in Rtx-6 cells. In contrast, 20 nM estradiol had no effect on the uptake of DOX-TEG-TAM by ER-negative, MDA-MB-435 cells (data not shown).

Detection of AEBS in MCF-7/Adr and MDA-MB-435 Cell Lines. An exhaustive search of the literature uncovered no indication of the presence or expression level of AEBS in MCF-7/Adr and MDA-MB-435 cell lines. There is evidence for the presence of AEBS in MCF-7 and MDA-MB-231 cell lines, and the expression level has been reported as 140000 sites/cell and 82000 sites/cell for MCF-7 (ER^+) and MDA-MB-231 (ER^-), respectively.[36] AEBS have been reported to be present

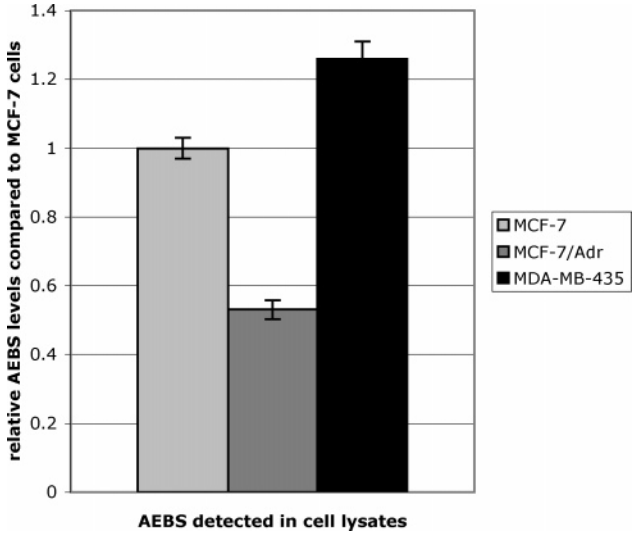

Figure 8. Relative concentration of AEBS in MCF-7, MCF-7/Adr, and MDA-MB-435 cell lysates.

in breast cancer cells independent of ER expression, with levels typically higher in ER^+ cell lines.[36,37]

MCF-7/Adr and MDA-MB-435 cell lysates were prepared in the same manner as the MCF-7 lysate utilized for AEBS binding assays. MCF-7, MCF-7/Adr, and MDA-MB-435 cell lysates containing 5 nM ^{3}H-tamoxifen were incubated in the presence and absence of 5000 nM cold tamoxifen. Additionally, cold estradiol (1000 nM) was added to every sample to saturate the ER present in the low speed lysate. Total lysate binding was measured for each cell lysate in the absence of cold tamoxifen, while nonspecific binding was measured in the presence of 1000-fold cold tamoxifen. The difference between total binding and nonspecific binding is, by definition, the AEBS specific binding. The ratio of AEBS specific binding for MCF-7/Adr and MDA-MB-435 lysates relative to the AEBS specific binding for MCF-7 lysate is presented in Figure 8. MCF-7/Adr cell lysate contained about 53% of the AEBS present in the MCF-7 cell lysate. MDA-MB-435 cell lysate contained 126% of the AEBS present in the MCF-7 cell lysate.

In conclusion, the enhanced uptake measured by flow cytometry (Figure 2) and fluorescence microscopy (Figure 4) experiments support the hypothesis that DOX-TEG-TAM targeting is mediated through the antiestrogen binding site as well as the ER. In addition to DOX-TEG-TAM retaining roughly 60% of the AEBS binding affinity of the targeting group for AEBS (Figure 5),

DOX-TEG-TAM is taken up and retained to a significantly greater extent (up to 6-fold) than DOX and DOXSF. When MDA-MB-435 cells are treated with DOX or DOXSF for various times up to 3 h, anthracycline fluorescence appears nuclear, while DOX-TEG-TAM remains in the cytosol following treatment for times less (5−40 min) than the 60 min half-life for hydrolysis. From 40 to 60 min, DOX-TEG-TAM fluorophore appears to localize at a cytosolic site, and following release from the trigger/targeting group, the DOX fluorophore appears nuclear.

Perhaps the most compelling evidence for the role of AEBS and ER in the targeting mechanism comes from the competition experiments (Figures 3 and 7). The uptake of DOX-TEG-TAM by AEBS-positive, ER-negative MDA-MB-435 cells was substantially reduced in the presence of tamoxifen, an AEBS ligand, and by AEBS-negative, ER-positive Rtx-6 cells, in the presence of estradiol, a specific ER ligand. The competitive inhibition was observed to be dose dependent, with DOX-TEG-TAM uptake reduced by over 50% in the presence of 20-fold tamoxifen or 0.02-fold estradiol, respectively, to a level similar to untargeted DOXSF. In summary, the data support the hypothesis that the DOX-TEG-TAM targeting mechanism involves an interaction with the antiestrogen binding site and ER.

Experimental Section

General. The concentrations of test compounds were determined spectrophotometrically by UV/vis absorption with a Hewlett-Packard 8452A diode array spectrophotometer interfaced to an Agilent ChemStation data system as described for each biological assay. Flow cytometric measurements were performed using a Becton Dickinson FACScan (Franklin Lakes, NJ) flow cytometer. Fluorescence microscopy was performed using a Leica DM IRB fluorescence microscope with an ebq 100 mercury lamp power source (E Licht Company, Denver, CO) equipped with a Photometrics Sensys (Tucson, AZ) digital CCD camera system. Fluorescence images were processed using IPLab Spectrum software. Centrifugation of AEBS cell lysates was accomplished with a Beckman J2-21 centrifuge. Cell lysis was performed with a Misonix Sonicator Ultrasonic processor fitted with a microtip.

^{3}H-Tamoxifen was obtained from Amersham Pharmacia Biotech (Buckinghamshire, England). Cold tamoxifen and estradiol were all obtained from Sigma (St. Louis, MO). Doxorubicin hydrochloride was purchased from Hande Tech (Houston, TX), and DOX−saliform and DOX-TEG-TAM were synthesized as previously described.[17,22] Complete-Mini protease inhibitor cocktail tablets were obtained from Boehringer Mannheim (Indianapolis, IN). Cell lysate total protein was measured with a Micro Protein Determination kit from Sigma Diagnostics (Dorset, England). Liquid scintillation counting was performed using a Packard (Downers Grove, IL) Tri-Carb 1600 TR liquid scintillation analyzer. Econo-Safe biodegradable liquid scintillation cocktail was from Research Products International Corporation (Mount Prospect, IL).

All tissue culture materials were obtained from Gibco Life Technologies (Grand Island, NY) unless otherwise stated. MCF-7 and MDA-MB-231 cells were obtained from American Type Culture Collection (Rockville, MD). MCF-7/Adr doxorubicin-resistant cells were a gift from Dr. William W. Wells (Michigan State University, East Lansing, MI). MDA-MB-435 and Rtx-6 cells were generously provided by Dr. Renata Pasqualini (MD Anderson Cancer Center, Houston, TX) and Dr. Marc Poirot (Toulouse, France), respectively. MCF-7, MCF-7/Adr, and MDA-MB-231 cells were maintained in vitro by serial culture in RPMI 1640 medium supplemented with 10% fetal bovine serum (Gemini Bioproducts, Calbassas, CA), L-glutamine (2 mM), HEPES buffer (10 mM), penicillin (100 units/mL), and streptomycin (100 μg/mL). MDA-MB-435 cells were maintained in vitro by serial culture in DMEM medium supplemented with 5% fetal bovine serum, L-glutamine (2 mM), sodium pyruvate (1 mM), and nonessential amino acids and vitamins for minimum essential media. Rtx-6 cells were maintained in vitro by serial culture in RPMI 1640 medium supplemented with 5% FBS, L-glutamine (2 mM), HEPES buffer (10 mM), penicillin (100 units/mL), streptomycin (100 μg/mL), and 1.00 μM tamoxifen (Sigma, St. Louis, MO). Tamoxifen was excluded from the media when experiments were performed. Phenol red free media supplemented with L-glutamine was obtained from Sigma (St. Louis, MO). Cells were maintained at 37 °C in a humidified atmosphere of 5% CO_2 and 95% air.

Uptake and Release of DOX, DOXSF, and DOX-TEG-TAM. The uptake and release of DOX-TEG-TAM in breast cancer cells relative to DOX and untargeted DOXSF was performed as described with modifications.[29,30] Breast cancer cells in log phase growth were dissociated with trypsin-EDTA, counted, resuspended in media at 1.5×10^5 cells/mL, and plated into six well plates (450000 cells/well) and allowed to adhere overnight. The cells were treated with 0.5 μM DOX, DOXSF, or DOX-TEG-TAM for various amounts of time (20, 40, and 60 min). Drug treatment was accomplished by addition of 30 μL of 100× drug solution (50 μM) to 3 mL of medium which was mixed and immediately added to the cells. For each time point, the medium was removed, cells were trypsinized, and trypsinization was quenched with 3 mL of phenol red free RPMI 1640 medium (no serum) at 4 °C. Cells were pelleted by centrifugation at 300*g* for 5 min at 10 °C. The supernatant was decanted, and the cells were resuspended in 1 mL of serum-free and phenol red free RPMI 1640 medium and placed on ice.

For drug retention samples, the cells were treated for 1 h with 0.5 μM DOX, DOXSF, or DOX-TEG-TAM. Following drug treatment, the medium was removed and replaced with 3 mL of fresh, 37 °C, full (containing serum and phenol red indicator) cell medium and the cells were incubated for various times (0.5, 1, 3, and 6 h). Following the allotted release times, the cells were prepared as described above. Drug treatment was performed such that all cell samples would be prepared within 2 h. Previous work has demonstrated that no loss of fluorescence is observed from cells stored on ice for up to 4 h.[29]

The extent of drug uptake and retention was measured by flow cytometry on a Becton Dickinson FACScan (Franklin Lakes, NJ) flow cytometer. Cells were analyzed with excitation at 488 nm (15 mW Ar ion laser), with emission monitored between 570 and 600 nm. Instrument settings were optimized for each cell line and held constant for all experiments; 10000 cells were analyzed for anthracycline fluorescence. The data are presented as the mean fluorescence for each condition with the background, drug-free cell fluorescence subtracted.

Tamoxifen Competition Experiments. MDA-MB-435 cells were treated with 0.5 μM DOX, DOXSF, or DOX-TEG-TAM in the absence and presence of the competitor, tamoxifen. Following drug treatment for 1 h, both anthracycline and tamoxifen were removed. The cell samples were prepared and analyzed by flow cytometry as described above.

Estradiol Competition Experiments. Rtx-6 cells were treated with 0.5 μM DOX-TEG-TAM in the absence and presence of the competitor, estradiol. Following drug treatment for 1 h, both anthracycline and estradiol were removed. The cell samples were prepared and analyzed by flow cytometry as described above.

Analysis of Drug Distribution by Fluorescence Microscopy. MDA-MB-435 cells in log phase growth were dissociated with trypsin-EDTA and counted. Cells were suspended in media at 8.3×10^4 cells/mL, and 3 mL of cell solution was aliquoted into 6 well plates and allowed to adhere overnight. The cells were treated with 0.5 μM DOX, DOXSF, or DOX-TEG-TAM for various amounts of time (5 min, 20 min, 40 min, 1 h, and 3 h). Drug treatment was accomplished by addition of 30 μL of 100× drug solution (50 μM) to 3 mL of medium which was mixed and immediately added to the cells.

Following drug treatment, the medium was removed, cells were washed once with 3 mL of serum-free and phenol red free RPMI 1640 at room temperature, and 3 mL of the same medium was then added back to each well. The cells were then immediately analyzed by fluorescence microscopy. Each condition was performed individually to minimize the amount of time between drug treatment and fluorescence detection.

Microscopic images of the cells were observed at a magnification of 40× and recorded with a Leica DM IRB fluorescence microscope equipped with a Photometrics Sensys digital CCD camera system. Cell images were observed with a shutter time of 0.05 s; fluorescence images were observed with a shutter time of 1.000 s. Drug fluorescence was observed at wavelengths above 590 nm with excitation between 515 and 560 nm. Fluorescence images were processed using IPLab Spectrum software.

Evaluation of DOX-TEG-TAM Binding Affinity to AEBS. The binding affinity of DOX-TEG-TAM (**2c**) relative to *E*/*Z*-4-OHT (**5**) was measured through competition assay with tritiated tamoxifen (^{3}H-TAM) through a procedure adapted from several sources.[34,37,38] MCF-7 cells were utilized as the AEBS source. Cells were cultured in six T-175 flasks to 90% confluence. To harvest, cells were washed with 10 mL of Hank's balanced salt solution and dissociated from the flasks with 2 mL of trypsin. Trypsinization was quenched with 10 mL of phenol red free RPMI medium supplemented with 10% dextran-coated charcoal (DCC) stripped fetal calf serum ("stripped medium"); cells from six T-175 flasks were combined and pelleted by centrifugation at 300*g* for 5 min at 25 °C. The supernatant was decanted, and the cells were resuspended in 50 mL of stripped medium and enumerated with a hemacytometer. The cells were then pelleted again by centrifugation, as described above. The supernatant was decanted, and the cells were suspended in pH 7.4 lysis buffer (10% v/v glycerol, 10 mM Tris, 1.5 mM EDTA, 0.5 mM dithiothreitol, 10 mM Na_2MoO_4, 1.0 mM phenylmethylsulfonyl fluoride, supplemented with Complete-Mini protease inhibitors) at 4 °C such that the cell density was 38 million cells per mL lysis buffer. Cells were lysed at 0 °C via sonication with a microtip set at maximum power for 10 cycles of 6 s on followed by 24 s off. The AEBS-enriched lysate was obtained by centrifugation of the homogenate at 12000*g* for 30 min at 4 °C. The supernatant was dispensed into 100 μL aliquots and stored at −70 °C. The lysate protein density was measured with a Sigma Diagnostics Total Protein kit; for all experiments the stock lysate was diluted such that the protein density was 2.0 mg/mL.

Competitive ligands were prepared as 120× solutions (50 nM working concentrations) in DMSO containing 1% acetic acid. Competitor concentrations were determined for ligands containing the DOX chromophore by optical density at 480 nm (ϵ = 11500 L/mol·cm). Three different concentrations (5 nM, 0.5 nM, and 0.05 nM) of tritiated tamoxifen were prepared as 240× solutions in DMSO containing 1% acetic acid. Cold estradiol (1 μM) was added to every sample to saturate the ER present in the low speed lysate; cold estradiol was prepared as a 240 μM (240×) stock solution to provide a 1 μM estradiol working concentration. Equal volumes of the 240× solutions of tritiated tamoxifen and cold estradiol were added together to provide 120× solutions of each ligand in DMSO containing 1% acetic acid. The 120× solutions were then diluted 1:10 in pH 7.6 TE (10 mM Tris, 1 mM EDTA) buffer to provide 12× solutions of ^{3}H-TAM/estradiol and competitors. Aliquots of cell lysate (100 μL) were thawed at 4 °C; 10 μL of 12× competitor was added, followed by 10 μL of 12× ^{3}H-TAM/estradiol at each of the three tritiated tamoxifen concentrations. Total binding was measured by addition of vehicle (DMSO containing 1% acetic acid) in the absence of competitor; ^{3}H-TAM binding inhibition was measured by addition of *E*/*Z*-4-OHT or DOX-TEG-TAM. Reaction lysates were vortexed vigorously and stored at 4 °C for 18 h.

Following incubation, unbound aromatic organics were stripped from the lysate by addition of 280 μL of DCC as a 2% w/v suspension in pH 7.6 TE buffer (10 mM Tris, 1.0 mM EDTA). Following the addition of the DCC, the reaction lysates were vortexed and stored on ice for 15 min, with vortexing every 5 min. DCC was pelleted by centrifugation at 3000*g* for 10 min at 4 °C; 300 μL of lysate supernatant was transferred to scintillation vials containing 4 mL of Econosafe biodegradable scintillation cocktail. The vials were then vortexed vigorously, and each sample was counted for 5 repetitions of 3 min counts. This counting protocol was then repeated to ensure reproducibility. Scintillation counting background was subtracted from all measurements. The percentage of targeting group binding for DOX-TEG-TAM relative to targeting group alone was determined by comparison of the reduction of tritiated tamoxifen at each concentration. Scintillation counting was performed in triplicate, and each competitor was assayed in duplicate. Error bars represent one standard deviation for the percentage DOX-TEG-TAM binding relative to *E*/*Z*-4-OHT at three different tritiated tamoxifen concentrations.

Growth Inhibition of Rtx-6 Cells. The concentration inhibiting half the growth (IC_{50}) was determined as previously described with minor modifications.[13] All compounds were solubilized in dimethyl sulfoxide containing 1% v/v acetic acid. The concentrations of all 100× DMSO/1% AcOH drug solutions were determined spectrophotometrically by absorbance at 480 nm (ϵ = 11500 L/mol·cm). Drug treatment lasted 4 h; and cells were cultured until the control wells had achieved 80% confluence (typically 4−5 days). Every experiment was performed six times for each drug level and controls. Error bars represent one standard deviation about the mean for the six wells per lane measured for each drug concentration.

Detection of AEBS in MCF-7/Adr and MDA-MB-435 Cells. The presence of AEBS was measured through the binding of ^{3}H-tamoxifen in MCF-7, MCF-7/Adr, and MDA-MB-435 cell lysates. MCF-7/Adr and MDA-MB-435 cell lysates were prepared as described above for the AEBS binding assay. All three cell lysates were diluted to achieve a uniform protein density of 2.0 mg/mL.

Binding ligands were prepared as 120× solutions in DMSO containing 1% acetic acid and delivered to cell lysates as described above. MCF-7, MCF-7/Adr, and MDA-MB-435 cell lysates containing 5 nM ^{3}H-tamoxifen were incubated in the presence and absence of 5000 nM cold tamoxifen. Additionally, cold estradiol (1000 nM) was added to every sample to saturate the ER present in the low speed lysate; cold estradiol was prepared as described above. Total lysate binding was measured for each cell lysate in the absence of cold tamoxifen, while nonspecific lysate binding was measured in the presence of cold tamoxifen. The difference between total binding and nonspecific binding is, by definition, the AEBS specific binding. Following incubation, the cell lysates were prepared for liquid scintillation counting as described above. The ratio of AEBS specific binding for MCF-7/Adr and MDA-MB-435 relative to the AEBS specific binding for MCF-7 is presented. Error bars represent one standard deviation from the mean of the scintillation counting statistics.

Acknowledgment. The authors would like to thank the National Cancer Institute of the NIH (CA-92107) for financial support. We also thank Dr. Renata Pasqualini (MD Anderson Cancer Center, Houston, TX), Dr. Marc Poirot (Toulouse, France), and Dr. William Wells (Michigan State University, East Lansing, MI) for generously providing MDA-MB-435, Rtx-6, and MCF-7/Adr cells, respectively, and Theresa Nahreini for help with the cell experiments. P.J.B. thanks the Colorado Institute for Research in Biotechnology (CIRB) and the U.S. Army Breast Cancer Research Program (DAMD 17-01-1-0213) for predoctoral fellowships. T.H.K. thanks the University of Colorado Council for Research and Creative Work for a faculty fellowship.

References

(1) Koutsilieris, M.; Reyes-Moreno, C.; Choki, I.; Sourla, A.; Doillon, C.; et al. Chemotherapy cytotoxicity of human MCF-7 and MDA-MB-231 breast cancer cells is altered by osteoblast-derived growth factors. *Mol. Med.* **1999**, *5*, 86−97.

(2) Gewirtz, D. A. A critical evaluation of the mechanisms of action proposed for the antitumor effects of the anthracycline antibiotics adriamycin and daunomycin. *Biochem. Pharmacol.* **1999**, *57*, 727−741.

(3) Doroshow, D. A. *Anthracyclines and anthracenediones*; Lippincott-Raven: Philadelphia, 1996; pp 409−434.

(4) Sklandanowski, A.; Konopa, J. Adriamycin and daunomycin induce programmed cell death (apoptosis) in tumour cells. *Biochem. Pharmacol.* **1993**, *46*, 375−382.

(5) Zeman, S. M.; Phillips, D. R.; Crothers, D. M. Characterization of covalent Adriamycin-DNA adducts. *Proc. Natl. Acad. Sci. U.S.A.* **1998**, *95*, 11561−11565.

(6) Wang, A. H. J.; Gao, Y. G.; Liaw, Y. C.; Li, Y. K. Formaldehyde cross-links daunorubicin and DNA efficiently: HPLC and X-ray diffraction studies. *Biochemistry* **1991**, *30*, 3812−3815.

(7) Luce, R. A.; Sigurdsson, S. T.; Hopkins, P. B. Quantification of formaldehyde-mediated covalent adducts of Adriamycin with DNA. *Biochemistry* **1999**, *38*, 8682−8690.

(8) Podell, E. R.; Harrington, D. J.; Taatjes, D. J.; Koch, T. H. Crystal structure of epidoxorubicin-formaldehyde virtual crosslink of DNA and evidence for its formation in human breast-cancer cells. *Acta Crystallogr.* **1999**, *D55*, 1516−1523.

(9) Taatjes, D. J.; Gaudiano, G.; Resing, K.; Koch, T. H. Alkylation of DNA by the anthracycline, antitumor drugs Adriamycin and Daunomycin. *J. Med. Chem.* **1996**, *39*, 4135−4138.

(10) Cutts, S. M.; Swift, L. P.; Rephaeli, A.; Nudelman, A.; Phillips, D. R. Sequence specificity of Adriamycin-DNA adducts in human tumor cells. *Mol. Cancer Ther.* **2003**, *2*, 661−670.

(11) Swift, L. P.; Cutts, S. M.; Rephaeli, A.; Nudelman, A.; Phillips, D. R. Activation of Adriamycin by the pH-dependent formaldehyde-releasing prodrug hexamethylenetetramine. *Mol. Cancer Ther.* **2003**, *2*, 189−198.

(12) Cutts, S. M.; Rephaeli, A.; Nudelman, A.; Hmelnitsky, I.; Phillips, D. R. Molecular basis for the synergistic interaction of Adriamycin with the formaldehyde-releasing prodrug pivaloyloxymethyl butyrate (AN-9). *Cancer Res.* **2001**, *61*, 8194−8202.

(13) Fenick, D. J.; Taatjes, D. J.; Koch, T. H. Doxoform and Daunoform: Anthracycline−formaldehyde conjugates toxic to resistant tumor cells. *J. Med. Chem.* **1997**, *40*, 2452−2461.

(14) Taatjes, D. J.; Fenick, D. J.; Koch, T. H. Epidoxoform: A hydrolytically more stable anthracycline−formaldehyde conjugate toxic to resistant tumor cells. *J. Med. Chem.* **1998**, *41*, 1306−1314.

(15) Cogan, P. S.; Koch, T. H. Rational design and synthesis of androgen receptor-targeted nonsteroidal anti-androgen ligands for the tumor-specific delivery of a doxorubicin−formaldehyde conjugate. *J. Med. Chem.* **2003**, *46*, 5258−5270.

(16) Dernell, W. S.; Powers, B. E.; Taatjes, D. J.; Cogan, P. S.; Gaudiano, G.; et al. Evaluation of the epidoxorubicin-formaldehyde conjugate, epidoxoform, in a mouse mammary carcinoma model. *Cancer Invest.* **2002**, *20*, 713−724.

(17) Burke, P. J.; Koch, T. H. Design, synthesis, and biological evaluation of doxorubicin−formaldehyde conjugates targeted to breast cancer cells. *J. Med. Chem.* **2004**, *47*, 1193−1206.

(18) Peekhaus, N. T.; Chang, T.; Hayes, E. C.; Wilkinson, H. A.; Mitra, S. W.; et al. Distinct effects of the antiestrogen Faslodex on the stability of estrogen receptors-alpha and -beta in the breast cancer cell line MCF-7. *J. Mol. Endocrinol.* **2004**, *32*, 987−995.

(19) Nikov, G. N.; Eshete, M.; Rajnarayanan, R. V.; Alworth, W. L. Interactions of synthetic estrogens with human estrogen receptors. *J. Endocrinol.* **2001**, *170*, 137−145.

(20) Mesange, F.; Sebbar, M.; Capdevielle, J.; Guillemot, J.-C.; Ferrara, P.; et al. Identification of two tamoxifen target proteins by photolabeling with 4-(2-morpholinoethoxy)benzophenone. *Bioconjugate Chem.* **2002**, *13*, 766−772.

(21) Kedjouar, B.; de Medina, P.; Oulad-Abdelghani, M.; Payre, B.; Silvente-Poirot, S.; et al. Molecular characterization of the microsomal tamoxifen binding site. *J. Biol. Chem.* **2004**, *279*, 34048−34061.

(22) Cogan, P. S.; Fowler, C. R.; Post, G. C.; Koch, T. H. Doxsaliform: A novel N-Mannich base prodrug of a doxorubicin formaldehyde conjugate. *Lett. Drug Des. Discovery* **2004**, *1*, 247−255.

(23) Katzenellenbogen, J. A.; Carlson, K. E.; Katzenellenbogen, B. S. Facile geometric isomerization of phenolic non-steroidal estrogens and antiestrogens: limitations to the interpretation of experiments characterizing the activity of individual isomers. *J. Steroid Biochem.* **1985**, *22*, 589−596.

(24) Mimnaugh, E. G.; Fairchild, C. R.; Fruehauf, J. P.; Sinha, B. K. Biochemical and pharmacological characterization of MCF-7 drug-sensitive and Adr multidrug-resistant human breast tumor xenografts in athymic mice. *Biochem. Pharmacol.* **1991**, *42*, 391−402.

(25) Godden, J.; Leake, R.; Kerr, D. J. The response of breast cancer cells to steroid and peptide growth factors. *Anticancer Res.* **1992**, *12*, 1683−1688.

(26) Gallois, L.; Fiallo, M.; Laigle, A.; Priebe, W.; Garnier-Sullerot, A. The overall partitioning of anthracyclines into phosphatidyl-containing model membranes depends neither on the drug charge nor the presence of anionic phospholipids. *Eur. J. Biochem.* **1996**, *241*, 879−887.

(27) Roche, C. J.; Thomson, J. A.; Crothers, D. M. Site selectivity of Daunomycin. *Biochemistry* **1994**, *33*, 926−935.

(28) Egorin, M. J.; Hildebrand, R. C.; Cimino, E. F.; Bachur, N. R. Cytofluorescence localization of Adriamycin and daunorubicin. *Cancer Res.* **1974**, *34*, 2243−2245.

(29) Taatjes, D. J.; Fenick, D. J.; Koch, T. H. Nuclear targeting and nuclear retention of anthracycline−formaldehyde conjugates implicates DNA covalent binding in the cytotoxic mechanism of anthracyclines. *Chem. Res. Toxicol.* **1999**, *12*, 588−596.

(30) Durand, R. E.; Olive, P. L. Flow cytometry studies of intracellular Adriamycin in single cells *in vitro*. *Cancer Res.* **1981**, *41*, 3489−3494.

(31) Taatjes, D. J.; Koch, T. H. Growth inhibition, nuclear uptake, and retention of anthracycline-formaldehyde conjugates in prostate cancer cells relative to clinical anthracyclines. *Anticancer Res.* **1999**, *19*, 1201−1208.

(32) Taatjes, D. J.; Fenick, D. J.; Gaudiano, G.; Koch, T. H. A redox pathway leading to the alkylation of nucleic acids by doxorubicin and related anthracyclines: application to the design of antitumor drugs for resistant cancer. *Cur. Pharm. Des.* **1998**, *4*, 203-218.

(33) Faye, J. C.; Jozan, S.; Redeuilh, G.; Baulieu, E. E.; Bayard, F. Physicochemical and genetic evidence for specific antiestrogen binding sites. *Proc. Natl. Acad. Sci. U.S.A.* **1983**, *80*, 3158−3162.

(34) Poirot, M.; Garnier, M.; Bayard, F.; Riviere, I.; Traore, M.; et al. The anti-proliferative properties of 4-benzylphenoxy ethanamine derivatives are mediated by the anti-estrogen binding site (ABS), whereas the anti-estrogenic effects of trifluopromazine are not. *Biochem. Pharmacol.* **1990**, *40*, 425−429.

(35) Delarue, F.; Kedjouar, B.; Mesange, F.; Bayard, F.; Faye, J. C.; et al. Modifications of benzylphenoxy ethanamine antiestrogen molecules: Influence affinity for antiestrogen binding sites (AEBS) and cell cytotoxicity. *Biochem. Pharmacol.* **1999**, *57*, 657−661.

(36) Reddel, R. R.; Murphy, L. C.; Hall, R. E.; Sutherland, R. L. Differential sensitivity of human breast cancer cell lines to the growth-inhibitory effects of tamoxifen. *Cancer Res.* **1985**, *45*, 1525−1531.

(37) Miller, M. A.; Katzenellenbogen, B. S. Characterization and quantitation of antiestrogen binding sites in estrogen receptor-positive and -negative human breast cancer cell lines. *Cancer Res.* **1983**, *43*, 3094−3100.

(38) Borras, M.; Jin, L.; Bouhoute, A.; Legros, N.; Leclercq, G. Evaluation of estrogen receptor, antiestrogen binding sites and calmodulin for antiestrogen resistance of two clones derived from the MCF-7 breast cancer cell line. *Biochem. Pharmacol.* **1994**, *48*, 2015−2024.

JM049496B